World Journal of Stem Cells

Submit a Manuscript: https://www.f6publishing.com

World J Stem Cells 2025 November 26; 17(11): 110381

DOI: 10.4252/wjsc.v17.i11.110381

ISSN 1948-0210 (online)

ORIGINAL ARTICLE

Basic Study

Cancer cell-dependent increase in senescence-like populations following exosome treatment from bone marrow and induced pluripotent stem cell-derived mesenchymal stem cells

Nidaa A Ababneh, Sura Nashwan, Razan AlDiqs, Mohammad A Ismail, Ahmed A Abdulelah, Anas H A Abu-Humaidan, Lina AlQirem, Khairallah Al-Abdallat, Talal Al-Qaisi, Tareq Saleh, Abdalla Awidi

Specialty type: Cell and tissue engineering

Provenance and peer review: Unsolicited article; Externally peer reviewed.

Peer-review model: Single blind

Peer-review report's classification

Scientific Quality: Grade A, Grade A, Grade A

Novelty: Grade A, Grade A, Grade A

Creativity or Innovation: Grade A, Grade B, Grade B

Scientific Significance: Grade A, Grade A, Grade A

P-Reviewer: Ke QH, PhD, Adjunct Associate Professor, Chief Physician, China; Kudo C, MD, Japan

Received: June 7, 2025

Revised: July 29, 2025

Accepted: October 9, 2025

Published online: November 26, 2025

Processing time: 173 Days and 4.7 Hours

Nidaa A Ababneh, Sura Nashwan, Mohammad A Ismail, Abdalla Awidi, Cell Therapy Center, University of Jordan, Amman 11942, Jordan

Razan AlDiqs, Department of Allied Sciences, Faculty of Arts and Sciences, Al-Ahliyya Amman University, Amman 19111, Jordan

Mohammad A Ismail, South Australian ImmunoGENomics Cancer Institute, Adelaide Medical School, University of Adelaide, Adelaide 5005, Australia

Ahmed A Abdulelah, Lina AlQirem, School of Medicine, University of Jordan, Amman 11942, Jordan

Ahmed A Abdulelah, Royal Papworth Hospital NHS Foundation Trust, Royal Papworth Hospital, Cambridge CB2 0AY, United Kingdom

Anas H A Abu-Humaidan, Department of Pathology, Microbiology and Forensic Medicine, School of Medicine, University of Jordan, Amman 11942, Jordan

Lina AlQirem, University of Arkansas for Medical Sciences, Arkansas City, KS 72205, United States

Khairallah Al-Abdallat, Bone Marrow Transplantation Unit, Jordan University Hospital, Amman 11942, Jordan

Khairallah Al-Abdallat, Abdalla Awidi, Hemostasis and Thrombosis Laboratory, School of Medicine, University of Jordan, Amman 11942, Jordan

Talal Al-Qaisi, Department of Biomedical Sciences, College of Health Sciences, Abu Dhabi University, Abu Dhabi 59911, United Arab Emirates

Tareq Saleh, Department of Pharmacology & Therapeutics, College of Medicine & Health Sciences Manama, Arabian Gulf University, Manama 329, Bahrain

Tareq Saleh, Department of Pharmacology and Public Health, Faculty of Medicine, The Hashemite University, Zarqa 13133, Jordan

Abdalla Awidi, Department of Hematology and Oncology, Jordan University Hospital, Amman 11942, Jordan

Corresponding author: Nidaa A Ababneh, Associate Professor, Cell Therapy Center, University of Jordan, Queen Rania Street, Amman 11942, Jordan. n.ababneh@ju.edu.jo

Abstract

BACKGROUND

Mesenchymal stem cell (MSC) extracellular vesicles, particularly exosomes (Exos), are gaining recognition as promising therapeutic tools for cancer due to their capacity to modulate tumor cell biology. Induced pluripotent stem cell-derived MSCs (iMSCs) revealed therapeutic characteristics compared with conventional MSCs due to their proliferative capacity and enhanced differentiation potential.

AIM

To study the impact of Exos derived from iMSCs (iMSC-Exos) and bone marrow MSCs (BMSC-Exos) on PANC1 and MDA-MB-231 cancer cells.

METHODS

The iMSCs and BMSCs were characterized based on the International Society for Cellular Therapy (2006) criteria by verifying the expression of MSC-specific markers and their differentiation potential. Exos were isolated from 48-hour conditioned media using sequential ultracentrifugation and characterized based on size, morphology, and expression of surface markers including CD9, CD81, and CD63. PANC1 and MDA-MB-231 cells were treated with the isolated Exos, and their effects on cell proliferation, apoptosis, senescence, and invasion were assessed.

RESULTS

In PANC1 cells iMSC-Exos sustained antiproliferative activity for 48 hours (35% reduction, $P < 0.01$) while BMSC-Exos had a transient effect. In MDA-MB-231 cells, both Exos lowered proliferation significantly after 48 hours (~28% and ~22% reduction, $P < 0.05$). Notably, these antiproliferative effects were not associated with apoptosis, but an increase in senescence-like tumor cells was identified as the primary response with iMSC-Exos inducing approximately 2.3-fold higher number of senescence-associated β-galactosidase-positive cells compared with BMSC-Exos across both cancer cell lines. Tumor cell invasion was markedly inhibited in PANC1 and MDA-MB-231 cells in response to iMSC-Exos (~60% and ~45% reduction, respectively, $P < 0.001$), and only in PANC1 cells in response to BMSC-Exos.

CONCLUSION

iMSC-Exos effectively inhibited tumor proliferation and invasion *via* a senescence-like mechanism. These results indicated that iMSC-Exos could serve as a cell-free cancer therapy and merit further animal model evaluation.

Key Words: Bone marrow-derived stromal cells; Induced pluripotent stem cell-derived mesenchymal stem cells; Cell-free cancer therapy; Exosomes; Breast cancer; Pancreatic cancer; Senescence-associated secretory phenotype

Core Tip: This study explored the effects of exosomes (Exos) obtained from bone marrow mesenchymal stem cells (MSCs) and MSCs derived from induced pluripotent stem cells on pancreatic and triple-negative breast cancer cells. Exos obtained from MSCs derived from induced pluripotent stem cells exhibited a stronger and sustained antiproliferative effect by inducing a senescence-like state without apoptosis. In contrast, bone marrow MSC-derived Exos showed variable effects depending on cancer type. These findings highlight the importance of Exos source in determining therapeutic outcomes and suggest senescence induction as a key response to Exos exposure.

Citation: Ababneh NA, Nashwan S, AlDiqs R, Ismail MA, Abdulelah AA, Abu-Humaidan AHA, AlQirem L, Al-Abdallat K, Al-Qaisi T, Saleh T, Awidi A. Cancer cell-dependent increase in senescence-like populations following exosome treatment from bone marrow and induced pluripotent stem cell-derived mesenchymal stem cells. *World J Stem Cells* 2025; 17(11): 110381
URL: https://www.wjgnet.com/1948-0210/full/v17/i11/110381.htm
DOI: https://dx.doi.org/10.4252/wjsc.v17.i11.110381

INTRODUCTION

Bone marrow mesenchymal stem cells (BMSCs) were among the first and most thoroughly studied sources of mesenchymal stem cells (MSCs)[1]. Recognized for their multipotent differentiation capacity, BMSCs have been extensively applied in regenerative medicine, especially for the repair of bone, cartilage, and muscle tissues[2]. In

addition to their differentiation capacity, BMSCs also provide therapeutic benefits through the secretion of extracellular vesicles (EVs), particularly exosomes (Exos)[3]. These nanoscale, lipid-bilayer-enclosed vesicles (30-150 nm) contain proteins, lipids, RNA, and other bioactive molecules, facilitating intercellular communication and promoting a variety of biological processes[4].

Targeting cellular senescence has gained interest as a therapeutic strategy in cancer, given that senescent cells permanently cease dividing while often producing factors that can counter tumor growth. The senescence-associated secretory phenotype (SASP) can either inhibit or support tumor progression depending on the biological environment and timing. Despite growing interest the ability of Exos from MSCs to trigger senescence in cancer cells remains poorly understood, particularly regarding how the cellular source of Exos influences this response.

Exos derived from BMSCs (BMSC-Exos) contain a wide range of bioactive molecules that promote tissue repair and modulate immune and tumor regulation. Their anti-inflammatory properties and regenerative potential have been extensively investigated[5]. Additionally, BMSC-Exos are gaining interest in cancer research for their potential to influence the tumor microenvironment[6]. These Exos can carry various molecules, including microRNAs (miRNAs), cytokines, and growth factors, which can impact cancer cell growth, migration, and apoptosis. The ability of BMSC-Exos to modulate these processes makes them a promising therapeutic tool for cancer treatment[7].

Induced pluripotent stem cells (iPSCs)-derived MSCs (iMSCs) have recently gained attention as a promising stem cell type and are created by reprogramming adult somatic cells to adopt an MSC phenotype. iMSCs exhibit several characteristics like BMSCs but also retain certain advantages of iPSCs, such as increased plasticity and proliferative potential[8,9]. The reprogramming process may also confer enhanced therapeutic properties, including improved survival under stress conditions and potentially altered secretome profiles that could influence their anti-cancer effects. Exos derived from iMSCs (iMSC-Exos) have shown strong regenerative and immunomodulatory effects in preliminary studies due to their origin from reprogramed cells with a more pluripotent profile. However, their specific roles in various pathological settings, especially cancer, remain largely uninvestigated[10-12].

The PANC1 (pancreatic cancer) and MDA-MB-231 (breast cancer) cell lines are commonly used as cellular models to investigate cancer cell behavior and responses to treatments. These cell lines represent particularly aggressive cancer types with limited therapeutic options, making them relevant models for evaluating novel therapeutic approaches. Exos derived from MSCs, including BMSC-Exos and iMSC-Exos, may interact uniquely with cancer cells, affecting tumor growth, migration, and apoptosis[13-16]. Exploring these interactions offers valuable insights into how specific Exos populations can influence cancer progression and may highlight new therapeutic targets.

In this study, we examined how BMSC-Exos and iMSC-Exos affect key cancer cell behaviors, including viability, apoptosis, senescence, and invasion in PANC1 and MDA-MB-231 cell lines. By comparing the biological activity of Exos from these two sources, we aimed to identify functional differences and assess whether iMSC-Exos could serve as an equally effective or potentially superior alternative to BMSC-Exos for therapeutic applications.

MATERIALS AND METHODS

Cell culture

BMSCs were previously obtained from donors at the Cell Therapy Center, University of Jordan, in Amman, as outlined in reference[17]. The study received ethical approval from the Institutional Review Board at the Cell Therapy Center (Approval No. IRB/02/2021/4) and was conducted in accordance with the principles of the Declaration of Helsinki. Prior to use in experiments, all cell cultures were tested and confirmed to be free of mycoplasma contamination. Both iMSC and BMSC lines (passage 3) were maintained in cell culture media consisting of Eagle's minimum essential medium-alpha modification, supplemented with 10% fetal bovine serum (FBS), 1% L-glutamine, and 1% antibiotic-antimycotic solution (all from Gibco, NY, United States). For osteogenic induction cells were cultured in the same cell culture media described above, supplemented with 10 mmol/L dexamethasone, 50 μg/mL ascorbic acid 2-phosphate, and 10 mmol/L β -glycerophosphate (all from Carbosynth, United Kingdom). Adipogenic differentiation medium included cell culture media supplemented with 10 mmol/L dexamethasone, 500 μM IBMX, 0.2 mmol/L indomethacin, and 10 μg/mL insulin. The PANC1 (ATCC® CRL-1469™) and MDA-MB-231 (ATCC® HTB-26™) cell lines were maintained in RPMI medium with 10% FBS, 1% L-glutamine, and 1% antibiotic-antimycotic with media changes every 2 days.

Generation of iMSC-derived embryoid bodies

iMSCs were generated from iPSCs through embryoid body (EB) formation followed by directed differentiation as previously described[16]. Three iPSC lines, previously established at the Cell Therapy Center[18], were cultured in mTeSR medium on Matrigel-coated plates until reaching confluency. To initiate EB formation iPSCs were detached using 0.5 M EDTA, centrifuged, and transferred to ultra-low attachment plates containing MSC differentiation medium composed of alpha MEM supplemented with 15% FBS, 1% L-glutamine, and 1% antibiotic-antimycotic solution. After 2 days the medium was refreshed and supplemented with 10 μM retinoic acid (Sigma-Aldrich, MA, United States). On day 4 the medium was replaced with fresh medium containing 0.1 μM retinoic acid, which was withdrawn on day 6. By day 7 EBs were seeded onto Matrigel-coated plates and cultured in MSC differentiation medium to promote iMSC induction. On day 12 2.5 ng/mL basic fibroblast growth factor was added, and the cultures were maintained under standard conditions until confluency. The resulting iMSCs were expanded, passaged, and cryopreserved in liquid nitrogen for future applications.

Differentiation of iMSCs and BMSCs

As previously described[16] iMSCs and BMSCs were seeded in complete culture medium in 6-well plates at a density of 200000 cells per well. Once the cultures reached approximately 50% confluency, osteogenic or adipogenic differentiation was initiated by replacing the complete culture medium with the respective induction medium. For osteogenic differentiation cells were maintained for 21-28 days until calcium deposits became microscopically visible. For adipogenic differentiation cells were cultured for 14-21 days until the formation of intracellular lipid vacuoles was observed. Differentiation efficiency was assessed by staining with Alizarin Red to detect calcium deposition and Oil Red O to visualize lipid accumulation. All differentiated cultures were examined and imaged using the EVOS XL Core Imaging System.

Flow cytometric analysis of iMSCs and BMSCs surface markers

For surface marker characterization of iMSCs and BMSCs, cells were collected and resuspended at a density of 1×10^6 cells per sample in staining buffer (2% bovine serum albumin in 1 × PBS). Cell viability and single-cell suspensions were verified by trypan blue exclusion and manual counting. Cells were then stained using a panel of fluorescently labeled antibodies targeting MSC markers, including CD90-FITC, CD105-PerCP, CD73-APC, CD73-PE, and CD44-PE, following the manufacturer's instructions (BD Stemflow hMSC Analysis Kit, BD Biosciences, NJ, United States). Appropriate isotype controls were included to confirm staining specificity. After antibody incubation samples were washed twice with PBS and resuspended in 200 µL of PBS for analysis. Flow cytometry was performed on a BD FACS Canto II system (BD Biosciences, NJ, United States) using established gating strategies based on unstained and single-stained controls. First, an unstained cell suspension control was used to help set the forward and side scatter parameters. Stained cells with an isotype antibody control also were used to exclude false positive signals from the antibody marker. Finally, stained cells with a specific antibody marker were used to detect the percentage of the marker. All were read with distinct parameters depending on the cell suspension and fluorescence intensity. Initially, gating on forward and side scatter dot plot graphs was applied to exclude debris and identify the main cell population based on size and granularity. Then, fluorescence histograms for unstained control and isotype controls were gated to exclude false positive signals where inside the gate 0% of fluorescence. Lastly, this gate was applied to the fluorescence histogram for a specific antibody marker, revealing the positive percentage of that specified marker. Data were analyzed using BD FACSDiva software.

Exos isolation and purification

Conditioned media were harvested from iMSCs and BMSCs cultured for 48 hours in serum-free medium (SFM). Approximately 5×10^6 cells were seeded in 75 cm^2 flasks for this process. The collected media were initially centrifuged at 300 × *g* for 10 minutes and then a second spin at 2000 × *g* for 20 minutes to eliminate cellular debris. The supernatant was then filtered through 0.22 µm pore-size filters to ensure complete removal of residual cells and debris. Exos were isolated from the clarified media by ultracentrifugation at 100000 × *g* for 70 minutes at 4 °C. The resulting pellets were resuspended in filtered 1 × PBS, washed, and subjected to an additional ultracentrifugation step at the same speed and duration to improve purity. Purified iMSC-Exos and BMSC-Exos were resuspended in filtered PBS, and their protein content was quantified using the Micro BCA™ Protein Assay Kit (Thermo Fisher Scientific, MA, United States) per the manufacturer's instructions. The Exos concentrations were adjusted to a final concentration of 1 mg/mL, aliquoted in sterile PBS, and stored at -80 °C until further use[16,19]. For all functional assays Exos were diluted to a final working concentration of 50 µg/mL.

Exos surface markers

Flow cytometry was used to evaluate the expression of exosomal markers. To prepare the samples approximately 100 µg of Exos were mixed with 4 µL of 4% sulfate latex beads (Invitrogen, CA, United States) for 15 minutes. The bead-Exos complexes were then blocked using a solution containing 1 M glycine (Sigma, Germany) and 2% bovine serum albumin (Abcam, United Kingdom) in 1 × PBS to prevent nonspecific binding. After blocking, the samples were incubated for 40 minutes with fluorophore-conjugated antibodies specific to the tetraspanin markers CD9 (A5488), CD81 (AF647), and CD63 (APC) (BD Biosciences, NJ, United States) with appropriate isotype controls. Following staining, each sample was brought to a final volume with 150 µL of PBS. The samples were analyzed on a BD FACS Canto II flow cytometer (BD Biosciences, NJ, United States), and data were processed using BD FACSDiva software.

Exos size distribution

Dynamic light scattering was used to assess the size distribution of Exos. Around 100 µg of Exos suspension was diluted in sterile, filtered PBS and analyzed using a Zetasizer Nano ZS instrument (Malvern Instruments, Worcestershire, United Kingdom). Each sample underwent three independent measurements with 10 runs per measurement to ensure consistency. The resulting data were interpreted using Zetasizer software version 7.11, following the manufacturer's standard analysis protocols.

Exos morphology

Transmission electron microscopy (TEM) was employed to examine the morphology of Exos. Briefly, 100 µg of Exos were fixed in 2% paraformaldehyde and carefully placed onto carbon-coated copper grids. The samples were then subjected to negative staining using uranyl-oxalate. Imaging was carried out using a Versa 3D FEI TEM operated at an acceleration voltage of 30 kV to visualize the characteristic shape and structure of the Exos.

Cellular uptake of Exos

To assess cellular uptake 200 μL of iMSC-Exos and BMSC-Exos were labeled with 5 μL of the fluorescent dye DiI (1 mmol/L, 1,1′-dioctadecyl-3,3,3′,3′-tetramethylindocarbocyanine perchlorate; Invitrogen, CA, United States), following the manufacturer's instructions[16]. The labeling reaction was carried out for 1 hours in the dark with gentle mixing. Then labeled Exos were diluted in 4 mL of PBS and ultracentrifuged at 110000 × *g* for 1.5 hours at 4 °C to remove excess dye and the resulting pellets were resuspended in 700 μL PBS. PANC1 and MDA-MB-231 cells were seeded in serum-free RPMI at a density of 1.5 × 10^5 cells per well and then 30 μL of DiI-labeled Exos (100 μg/mL) were added for 16 hours. After incubation, cells were washed and stained with 2 μL of 5-chloromethylfluorescein diacetate (5 mmol/L, Invitrogen, CA, United States) in 1 mL of media for 30 minutes at 37 °C to visualize the cytoplasm, and then cells were fixed using 4% paraformaldehyde for 15 minutes and counterstained with DAPI (Invitrogen, CA, United States) to visualize nuclei. They were mounted with an anti-fade reagent (Abcam, United Kingdom) and imaged with a Carl Zeiss inverted fluorescent microscope.

Cancer cell proliferation assay

The impact of Exos on the proliferation of PANC1, MDA-MB-231, and fibroblast cells was evaluated using the MTT assay. Cells were plated in 96-well plates at a density of 8 × 10^3 cells per well and incubated for 24 hours to allow attachment. Cell culture medium was replaced with serum-free RPMI, then cells were incubated with either iMSC-Exos or BMSC-Exos (50 μg/mL) for 24 hours or 48 hours. Following treatment, 10 μL of MTT reagent (Thiazolyl Blue Tetrazolium Bromide, ATCC, VA, United States) was added to each well, and the plates were incubated at 37 °C for 3 hours. To solubilize the resulting formazan crystals, 100 μL of stop solution was added. Absorbance was then recorded at 570 nm using a Cytation 5 multi-mode reader (BioTek, VT, United States).

Apoptosis assay

Apoptosis induction by Exos was assessed using an Annexin V-FITC/PI apoptosis detection kit (eBioscience™, Thermo Fisher Scientific, MA, United States). PANC1 and MDA-MB-231 cells were plated in 6-well plates at a density of 3 × 10^5 cells per well. After 24 hours the culture medium was replaced with SFM, and the cells were treated with 50 μg/mL of either iMSC-Exos or BMSC-Exos for 48 hours. Following treatment, the cells were collected, stained according to the manufacturer's protocol, and analyzed by flow cytometry using a BD FACS Canto II instrument (BD Biosciences, NJ, United States). The proportion of apoptotic cells was then quantified and compared between the different treatment groups.

Senescence assay

Senescence was evaluated using the Senescence Detection Kit (Abcam, United Kingdom)[16]. PANC1 and MDA-MB-231 cells were plated at a density of 3 × 10^5 cells per well and treated with 50 μg/mL of either iMSC-Exos or BMSC-Exos in serum-free RPMI for 48 hours. After treatment the cells were washed with 1 × PBS and fixed with the provided fixative solution for 15 minutes at room temperature. The fixed cells were then stained and incubated overnight at 37 °C. Finally, the cells were observed under a microscope to quantify the proportion of senescent cells.

Wound healing assay (scratch assay)

A wound healing (scratch) assay was conducted to evaluate the impact of Exos on the invasion of PANC1 and MDA-MB-231 cells[16]. Confluent monolayers grown in 6-well plates were scratched with a sterile 200 μL pipette tip to create a wound. After washing with PBS to remove cell debris, the cells were treated with 50 μg/mL of either iMSC-Exos or BMSC-Exos in SFM. Images of the wound area were taken at 0 hour, 9 hours, and 48 hours using an inverted microscope (EVOS, Thermo Fisher Scientific, MA, United States). The wound closure percentage was then determined using ImageJ software by measuring the wound area at each time point and calculating the closure relative to the initial wound size.

Statistical analysis

All experiments were performed in triplicate, and data are presented as mean ± SD. Statistical analyses were carried out using GraphPad Prism version 9.3.1 (GraphPad Software, CA, United States). To determine significance unpaired Student's *t*-tests or two-way analysis of variance followed by Bonferroni post hoc tests were applied. A P value of ≤ 0.05 was considered statistically significant. Significance levels are indicated as: $^aP \leq 0.05$, $^bP \leq 0.01$, $^cP \leq 0.001$, and $^dP \leq 0.0001$. Each experiment was independently repeated three times ($n = 3$).

RESULTS

iMSCs and BMSCs showed typical characteristics of stem cells

Flow cytometry was performed to characterize iMSCs and BMSCs by evaluating the expression of human MSC surface markers. Positive markers analyzed included CD90, CD105, CD73, and CD44 while a negative marker cocktail consisted of hematopoietic markers CD34, CD45, CD14, CD11b, CD79a, CD19, and HLA-DR. Both iMSCs and BMSCs showed strong expression of the positive markers with over 95% positivity for CD90 and CD105 and less than 2% expression of the negative markers, indicating minimal hematopoietic contamination. The absence of significant phenotypic variation between iMSCs and control MSCs validates the effective induction of mesenchymal lineage from iPSCs (Figure 1A and B). Moreover, both MSC types were induced to undergo osteogenic and adipogenic differentiation. The differentiation

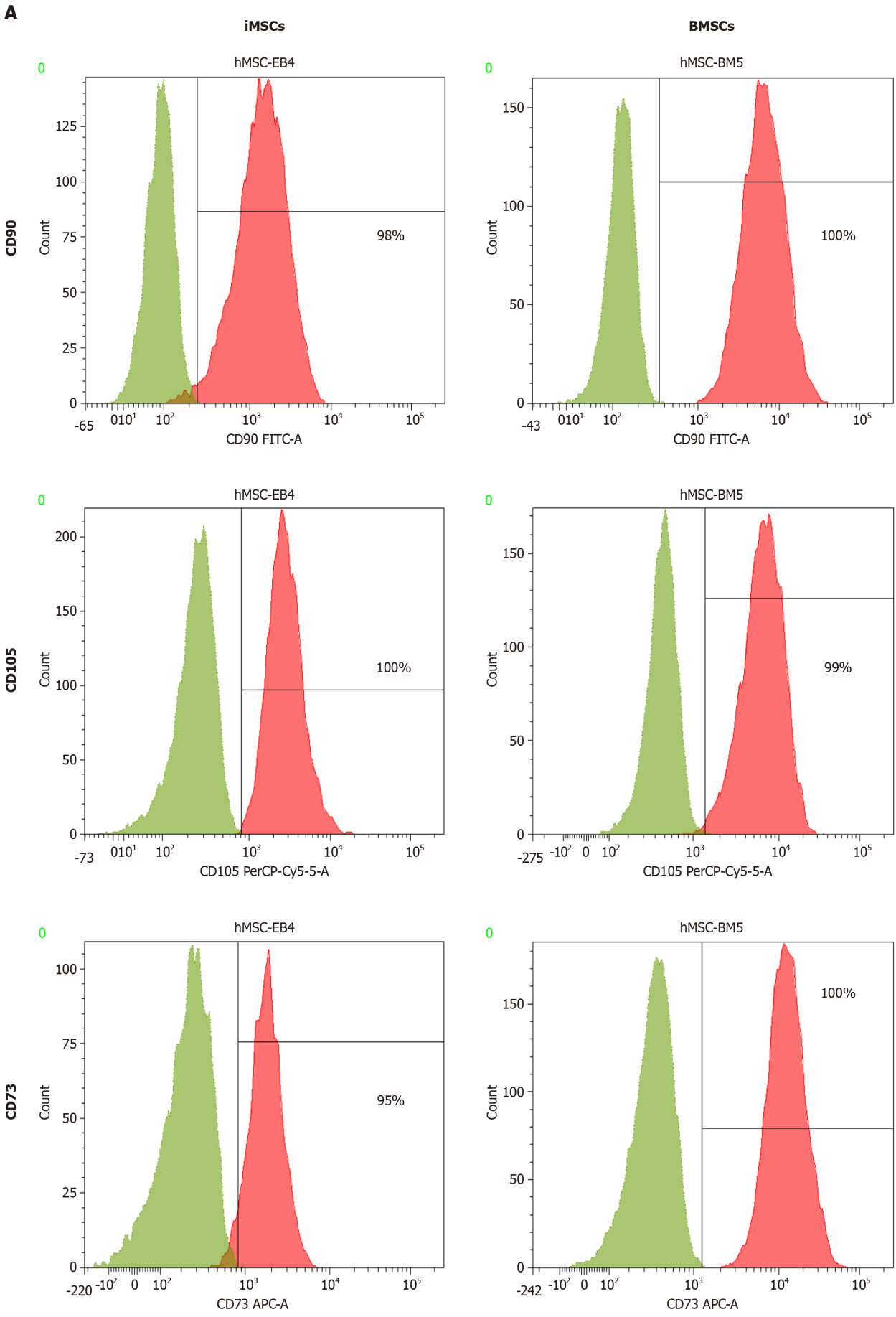
A
iMSCs
BMSCs
CD90
CD105
CD73
hMSC-EB4
hMSC-BM5
Count
98%
100%
99%
95%
CD90 FITC-A
CD105 PerCP-Cy5-5-A
CD73 APC-A

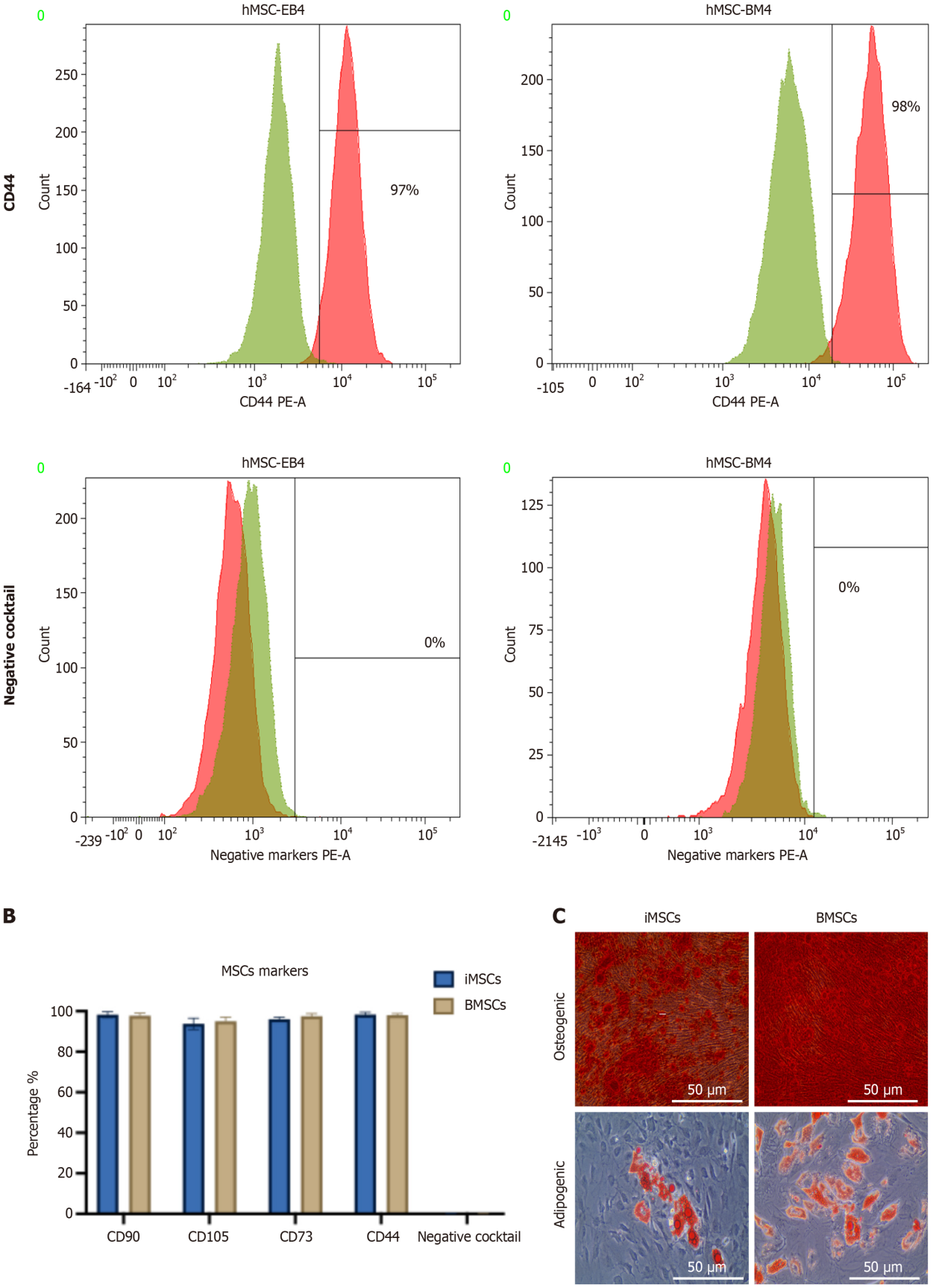

Figure 1 Characterization of induced pluripotent stem cell-derived mesenchymal stem cells and bone marrow mesenchymal stem cells. A: Flow cytometry analysis showed the expression of mesenchymal stem cell (MSC) positive surface markers (CD90, CD105, CD73, CD44) and negative hematopoietic lineage markers (CD34, CD45, CD14, CD11b, CD79a, CD19, HLA-DR) in both induced pluripotent stem cell-derived MSCs (iMSCs) and bone marrow MSCs (BMSCs); B: Quantitative comparison of human MSC surface marker expression between iMSCs and BMSCs; C: Osteogenic and adipogenic differentiation of iMSCs and BMSCs demonstrated by Alizarin Red staining (top panels) indicating calcium deposits and Oil Red O staining (bottom panels) showing lipid droplet

formation. Images of differentiated iMSC-derived cells are displayed in the lower left panels while those of BMSC-derived cells appear in the lower right panels (scale bar = 50 μm). iMSCs: Induced pluripotent stem cell-derived mesenchymal stem cells; BMSCs: Bone marrow mesenchymal stem cell; MSCs: Mesenchymal stem cells.

capacity was confirmed by Alizarin Red staining, which highlighted calcium deposits (Figure 1C), and Oil Red O staining, which indicated lipid accumulation (Figure 1C), with differentiation efficiencies exceeding 80%.

Characterization of isolated EVs showed typical Exos characteristics

Exosomal surface proteins CD9, CD81, and CD63 were assessed by flow cytometry following capture with sulfate-latex beads. Both iMSC-Exos and BMSC-Exos tested positive for these classical Exos markers (Figure 2A). Variation in the expression levels of these surface markers was observed between the two Exos populations. Notably, CD9 was expressed at significantly higher levels than CD81 and CD63 in both Exos groups (Figure 2B). No statistically significant differences in surface marker expression were observed between the two groups. The average percentages for iMSC-Exos were CD9 (98%), CD81 (81%), and CD63 (56%) while BMSC-Exos showed CD9 (100%), CD81 (83%), and CD63 (63%) (Figure 2C).

Dynamic light scattering analysis revealed that iMSC-Exos displayed a heterogeneous size distribution ranging from 32 nm to 145 nm, whereas BMSC-Exos exhibited a more uniform size profile centered around 150 nm (Figure 2D). TEM confirmed the characteristic cup-shaped morphology of both Exos populations. To evaluate Exos cellular uptake, DiI-labeled iMSC-Exos and BMSC-Exos were incubated with human dermal fibroblasts (HDFs) and human umbilical vein endothelial cells (Figure 2E and F, respectively). Fluorescent imaging showed efficient internalization of both Exos types with red DiI fluorescence localized to the perinuclear regions. To visualize cellular uptake the cytoplasm was labeled using 5-chloromethylfluorescein diacetate (green), and nuclei were stained with DAPI (blue). Both iMSC-Exos and BMSC-Exos were internalized by the target cells, supporting their potential role in mediating intercellular communication and cargo delivery.

Exos from iMSCs and BMSCs suppressed the proliferation of PANC1 and MDA-MB-231 cells with minimal apoptosis induction

To assess Exos uptake PANC1 and MDA-MB-231 cells were treated with DiI-labeled iMSC-Exos or BMSC-Exos and imaged after 12 hours using fluorescence microscopy. The red fluorescence was predominantly observed in the perinuclear regions of both cancer cell lines, confirming effective internalization (Figure 3A and B). Immunofluorescence images further demonstrated the presence of red fluorescent particles near the nuclei of PANC1 and MDA-MB-231 cells, indicating successful Exos uptake (Figure 3A and B).

For the evaluation of proliferation, PANC1, MDA-MB-231, and HDF cells were treated with iMSC-Exos or BMSC-Exos for 24 hours and 48 hours. MTT assays revealed a significant decrease in PANC1 cell proliferation at both timepoints with both Exos types with no notable difference between iMSC-Exos and BMSC-Exos (Figure 3C). MDA-MB-231 cells exhibited a decrease in proliferation after 24 hours of Exos treatment; however, this inhibitory effect was diminished by 48 hours, indicating a transient response (Figure 3D). In contrast, HDFs showed no significant change in proliferation (Figure 3E), suggesting that the antiproliferative effects of the Exos were partly selective for tumor cells.

To further evaluate the influence of iMSC-Exos and BMSC-Exos on apoptosis, Annexin V-FITC/PI staining followed by flow cytometry was performed after 48 hours of Exos treatment. In PANC1 cells, no significant changes were observed in early or late apoptosis or necrosis compared with serum-free controls. Notably, an increase in viable cell populations was observed following treatment with either Exos type (Figure 3F). Similarly, no significant changes in apoptotic populations were detected in MDA-MB-231 cells (Figure 3G), indicating that the observed growth suppression occurs independently of apoptotic mechanisms.

Antiproliferative effects of Exos were associated with an increased senescence-like cell population

Senescence induction was assessed by quantifying senescence-associated beta-galactosidase (SA-βGal)-positive cells (blue staining) in PANC1, MDA-MB-231, and fibroblast (control) cells following 48 hours of treatment with iMSC-Exos or BMSC-Exos. Representative images for PANC1 and MDA-MB-231 cells are shown in Figure 4A and B, respectively. In PANC1 cells, iMSC-Exos significantly increased the proportion of SA-βGal-positive cells compared with both the SFM control and BMSC-Exos (~2.3-fold increase, $P < 0.01$), while BMSC-Exos notably decreased senescent cell number relative to the SFM control (Figure 4C). In contrast, Exos exposure of MDA-MB-231 cells resulted in a greater increase in senescent cell number for both iMSC-Exos and BMSC-Exos compared with the SFM control. iMSC-Exos induced a higher percentage of SA-βGal-positive cells than BMSC-Exos (~1.8-fold *vs* ~1.4-fold increase respectively, P value < 0.05) (Figure 4D). This rise in SA-βGal-positive cells was associated with reduced cell proliferation without the induction of apoptosis.

Reduction in invasion rate of PANC1 cells by both Exos types and of MDA-MB-231 cells by iMSC-Exos

A wound healing (scratch) assay was conducted on PANC1 and MDA-MB-231 cells to assess wound healing at 0 hour, 9 hours, and 48 hours post-scratch. Microscopic images were captured to monitor cell invasion in PANC1 (Figure 5A) and MDA-MB-231 (Figure 5B) cultures. In PANC1 cells, treatment with both iMSC-Exos and BMSC-Exos significantly impaired invasion compared with the SFM control at both 9 hours and 48 hours (Figure 5C). In MDA-MB-231 cells, iMSC-Exos reduced invasion more effectively than BMSC-Exos at 9 hours and showed a significant inhibitory effect compared with both BMSC-Exos and the SFM control at 48 hours (Figure 5D).

A

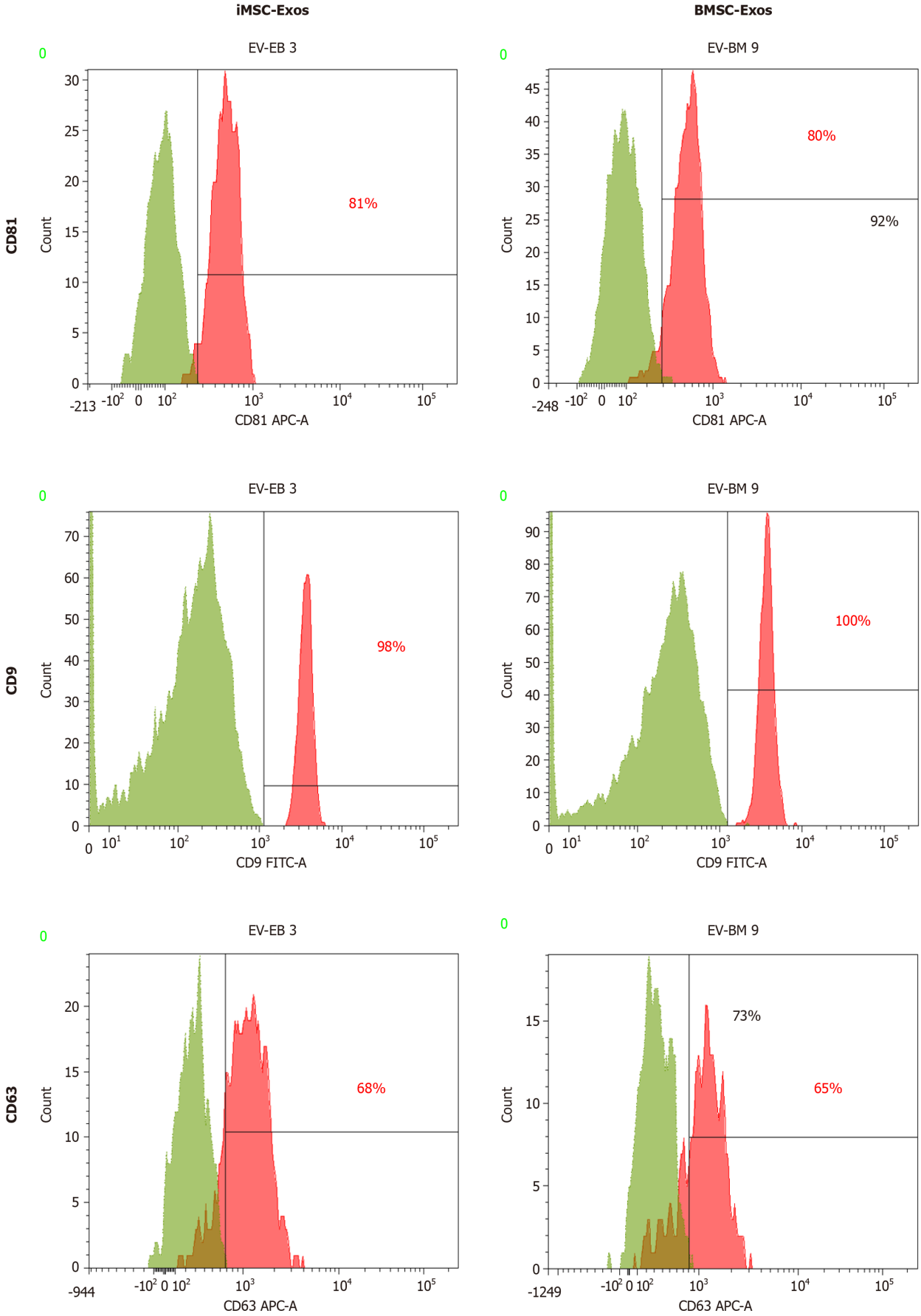
iMSC-Exos
BMSC-Exos
EV-EB 3
EV-BM 9
CD81
CD9
CD63
Count
81%
80%
92%
98%
100%
68%
73%
65%
CD81 APC-A
CD9 FITC-A
CD63 APC-A

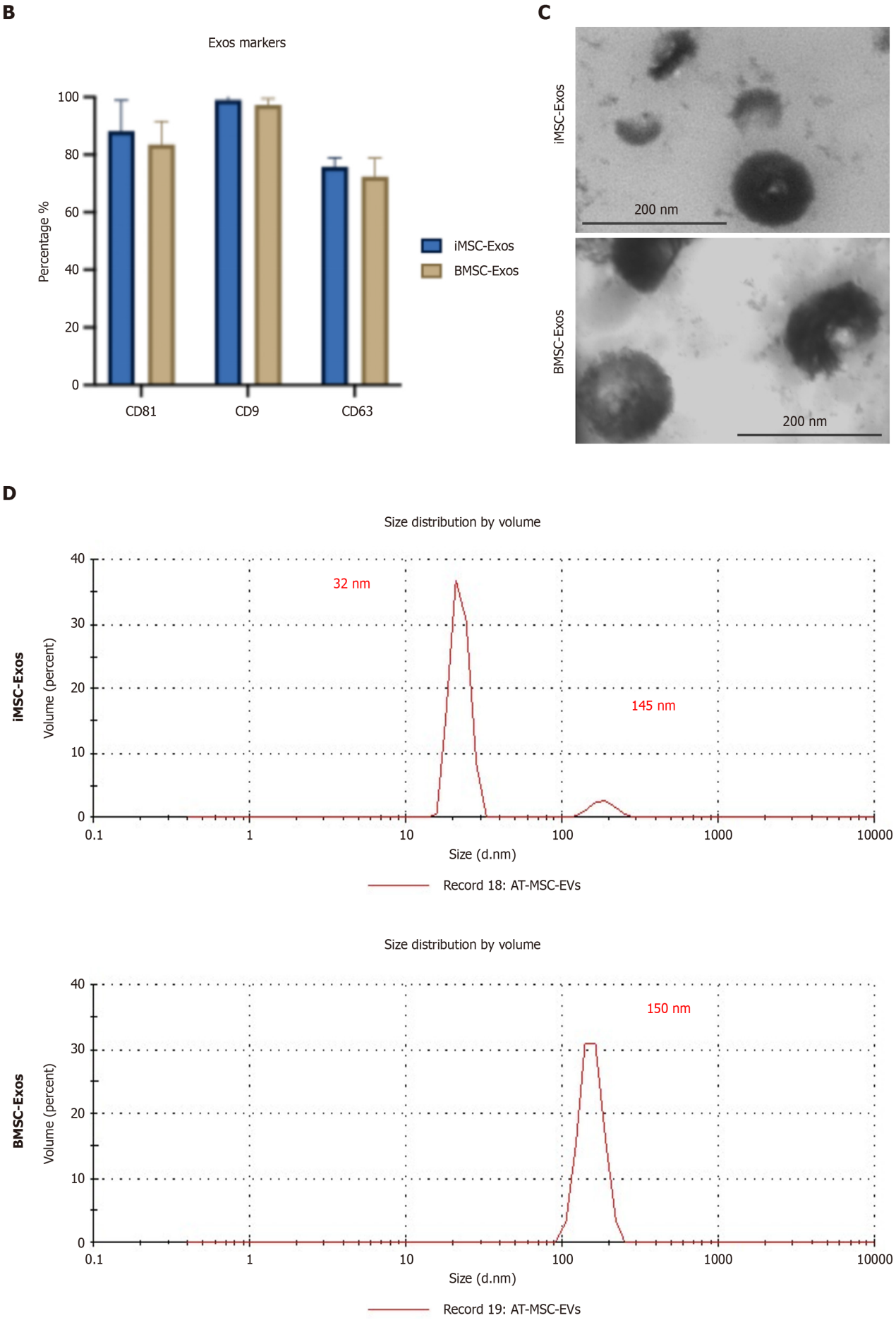
B
Exos markers
Percentage %
100
80
60
40
20
0
CD81
CD9
CD63
iMSC-Exos
BMSC-Exos
C
iMSC-Exos
200 nm
BMSC-Exos
200 nm
D
Size distribution by volume
iMSC-Exos
Volume (percent)
32 nm
145 nm
Size (d.nm)
Record 18: AT-MSC-EVs
Size distribution by volume
BMSC-Exos
Volume (percent)
150 nm
Size (d.nm)
Record 19: AT-MSC-EVs

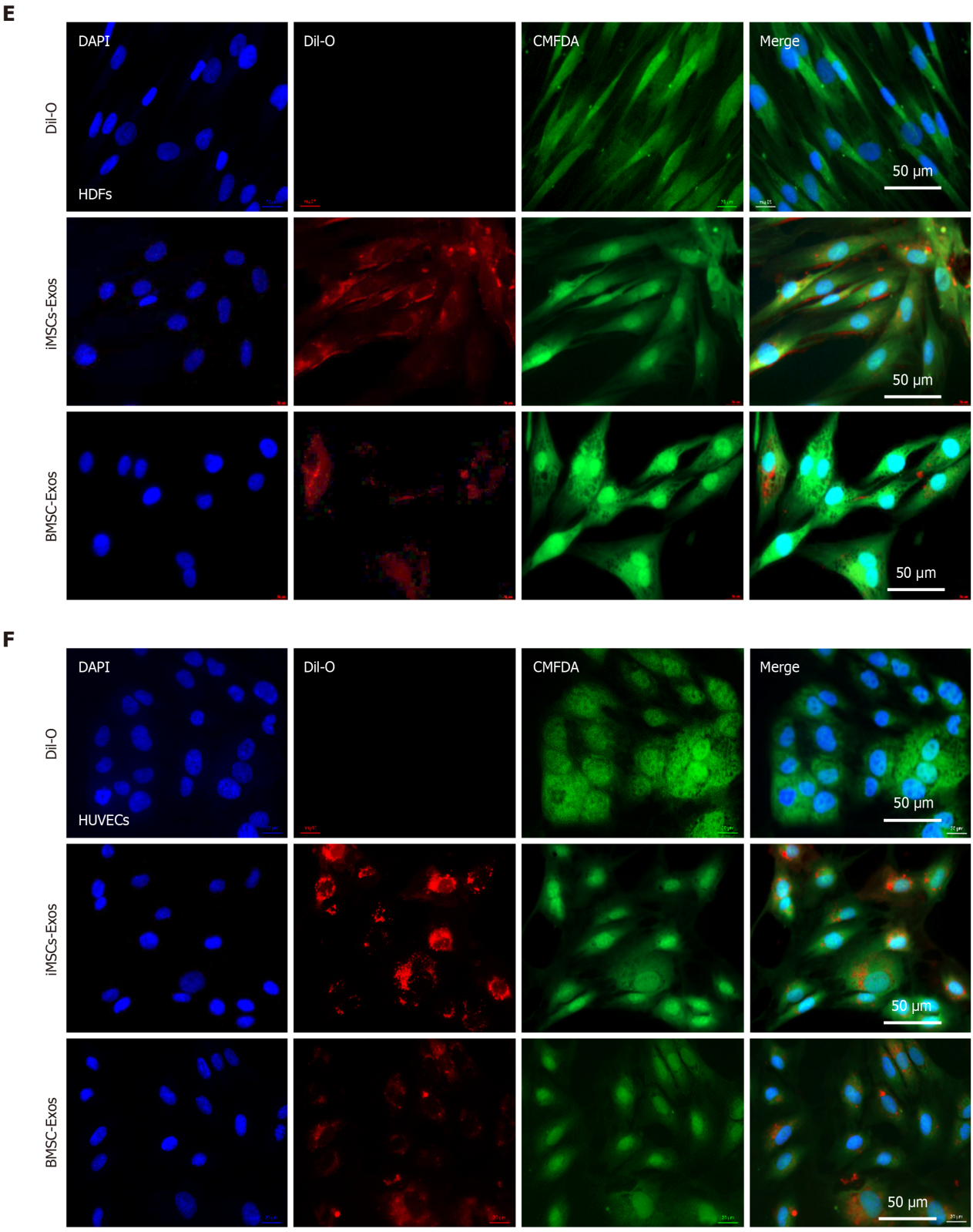

Figure 2 Characterization of exosomes derived from induced pluripotent stem cell-derived mesenchymal stem cells and bone marrow mesenchymal stem cells. A: Flow cytometry analysis showing expression of tetraspanin surface markers CD9, CD81, and CD63 on exosomes using sulfate-latex bead capture; B: Quantification of surface marker expression comparing exosomes derived from induced pluripotent stem cell-derived mesenchymal stem cells (iMSC-Exos) and exosomes derived from bone marrow mesenchymal stem cells (BMSC-Exos); C: Representative transmission electron microscopy images of iMSC-Exos (left) and BMSC-Exos (right). Scale bar = 200 nm; D: Dynamic light scattering profiles depicting size distribution of iMSC-Exos (top) and BMSC-Exos (bottom); E and F: Confocal microscopy images showing uptake of DiI-labeled exosomes (red) by human dermal fibroblasts (E) and human umbilical vein endothelial cells (F). Cells were costained with 5-chloromethylfluorescein diacetate (green) for the cytoplasm and DAPI (blue) for the nuclei. Scale bar = 50 μm. iMSC-Exos: Exosomes derived from induced pluripotent stem cell-derived mesenchymal stem cells; BMSC-Exos: Exosomes derived from bone marrow mesenchymal stem cell; Exos: Exosomes; HDFs: Human dermal fibroblasts; HUVECs: Human umbilical vein endothelial cells.

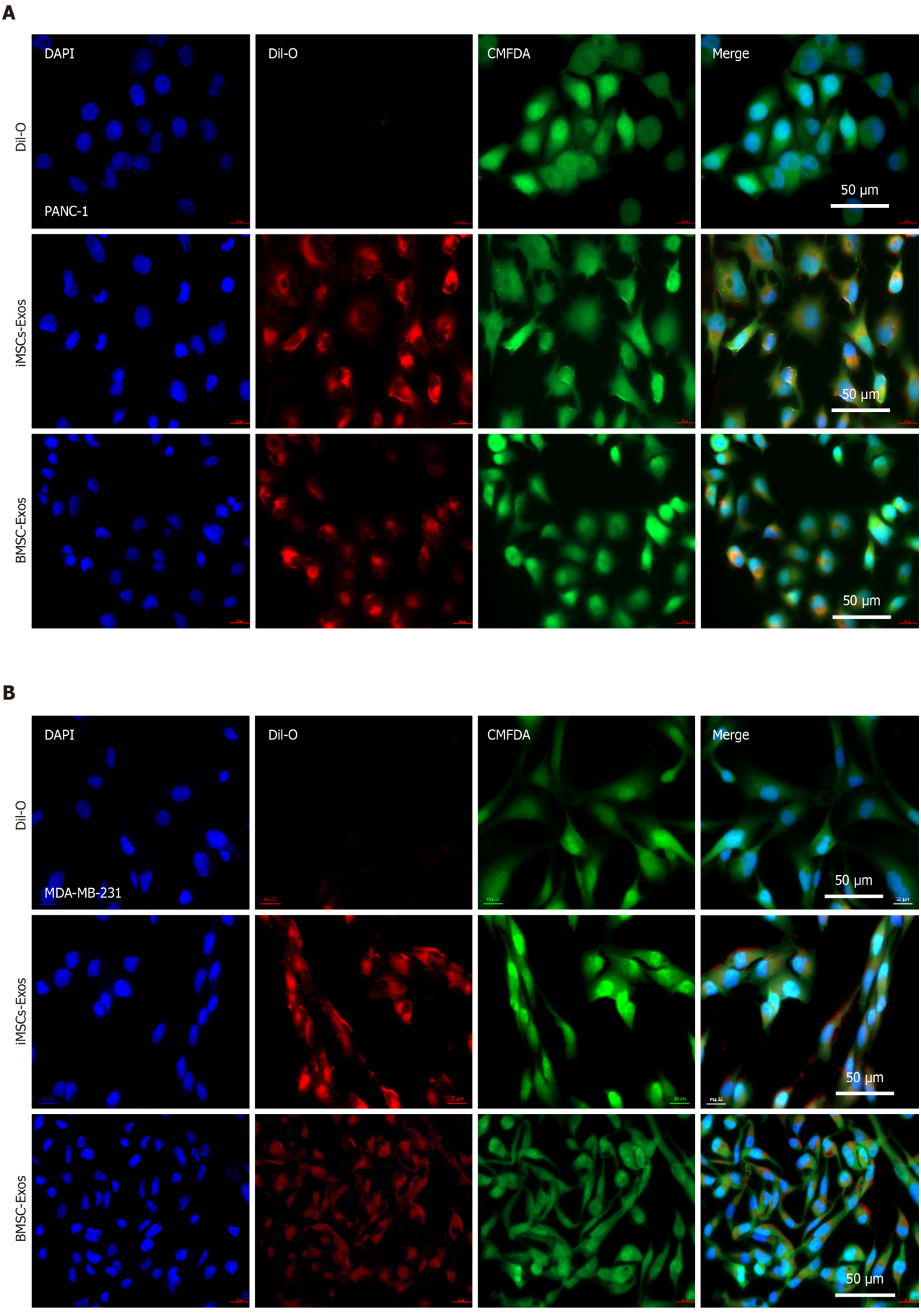
A
DAPI
Dil-O
CMFDA
Merge
Dil-O
PANC-1
50 μm
iMSCs-Exos
50 μm
BMSC-Exos
50 μm
B
DAPI
Dil-O
CMFDA
Merge
Dil-O
MDA-MB-231
50 μm
iMSCs-Exos
50 μm
BMSC-Exos
50 μm

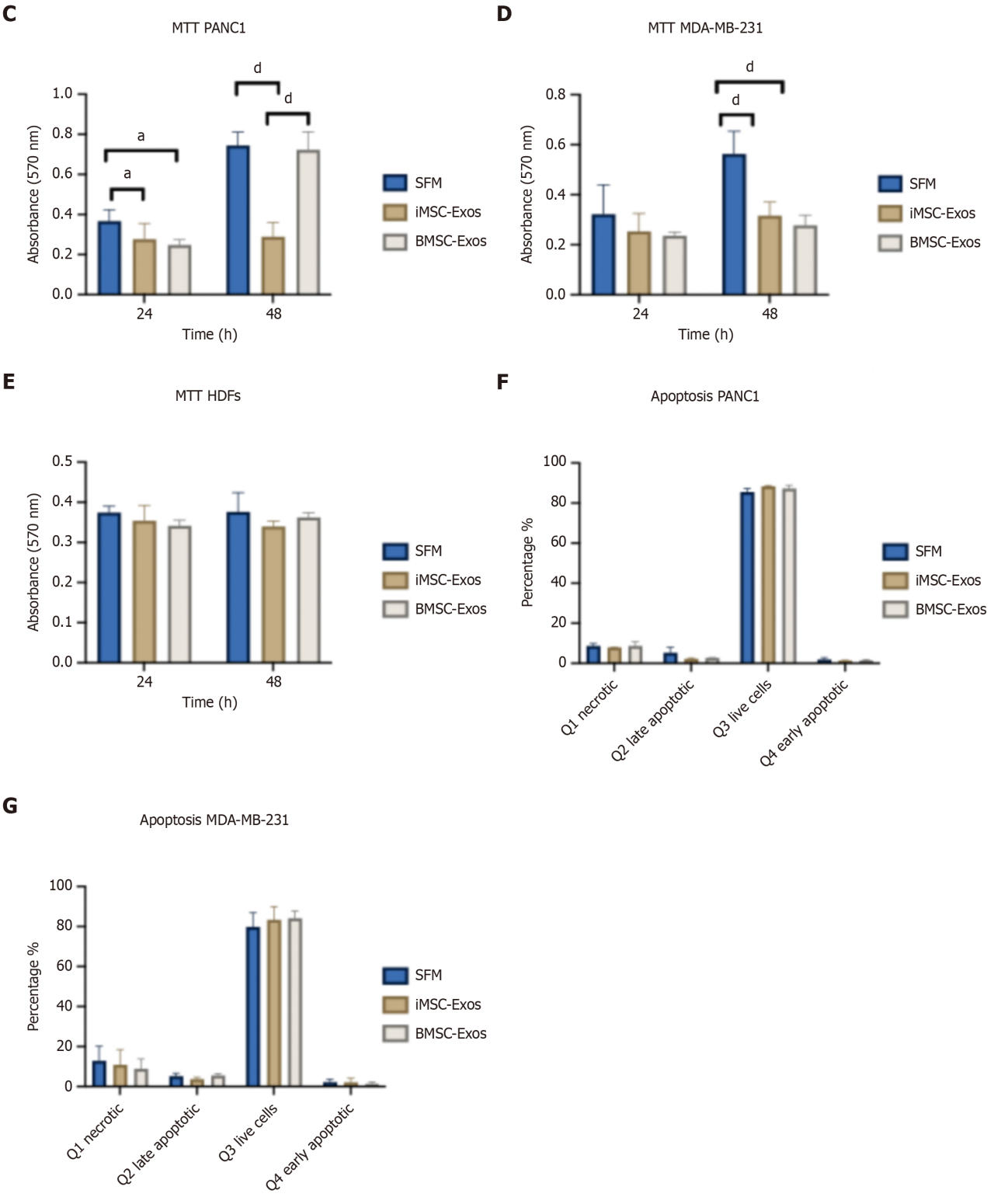

Figure 3 Assessment of exosome uptake, proliferation, and apoptosis in PANC1 and MDA-MB-231 cells with exosomes derived from induced pluripotent stem cell-derived mesenchymal stem cells or bone marrow mesenchymal stem cells. A and B: Fluorescence images showing internalization of DiI-labeled exosomes derived from induced pluripotent stem cell-derived mesenchymal stem cells and bone marrow mesenchymal stem cells by PANC1 (A) and MDA-MB-231 (B) cells after 12 hours of incubation. Red fluorescence indicates exosomes, scale bar = 50 μm; C-E: MTT assay results showing cell viability in PANC1 (C), MDA-MB-231 (D), and human dermal fibroblasts (E) following 24 hours and 48 hours of treatment with 50 μg/mL exosomes derived from induced pluripotent stem cell-derived mesenchymal stem cells or bone marrow mesenchymal stem cells; F and G: Flow cytometric analysis of apoptosis in PANC1 (F) and MDA-MB-231 (G) after 48-hour exposure to exosomes, using Annexin V-FITC/PI staining. Quadrants represent: Q1 = necrotic; Q2 = late apoptotic; Q3 = viable; and Q4 = early apoptotic cells. Data are presented as mean ± SD. $^{a}P \leq 0.05$, $^{d}P \leq 0.0001$. iMSC-Exos: Exosomes derived from induced pluripotent stem cell-derived mesenchymal stem cells; BMSC-Exos: Exosomes derived from bone marrow mesenchymal stem cell; SFM: Serum-free medium; HDF: Human dermal fibroblasts.

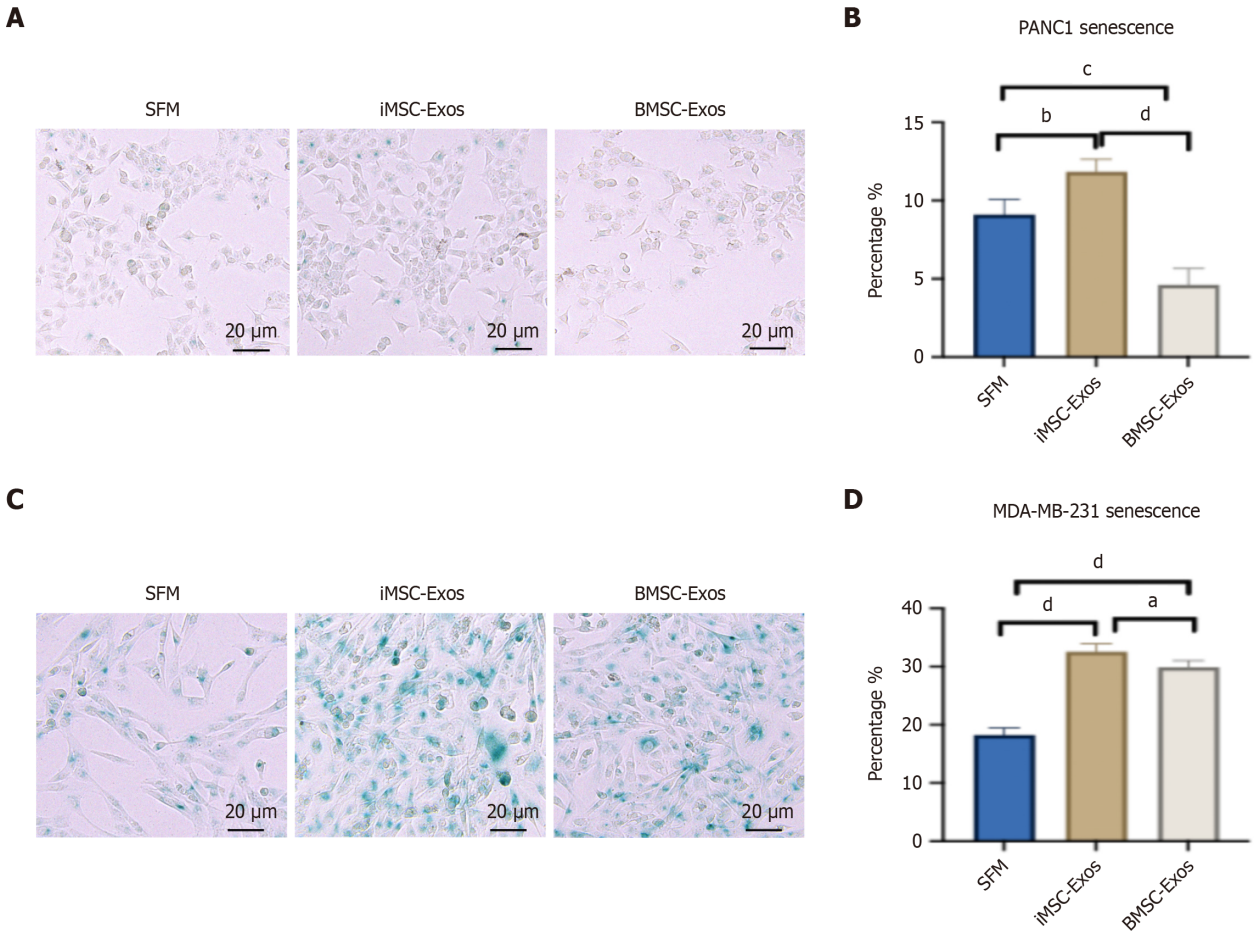

Figure 4 Senescence induction in PANC1 and MDA-MB-231 cells following treatment with exosomes derived from induced pluripotent stem cell-derived mesenchymal stem cells and bone marrow mesenchymal stem cells. A: Representative images of senescence-associated beta-galactosidase (SA-βGal)-stained PANC1 cells after 48 hours of treatment. Blue staining marks SA-βGal-positive senescent cells (scale bar = 20 μm); B: Quantification of SA-βGal-positive cells expressed as a percentage of the total cell population in PANC1 cultures; C: Representative images of SA-βGal-stained MDA-MB-231 cells after 48 hours of treatment. Blue staining marks SA-βGal-positive senescent cells (scale bar = 20 μm); D: Quantification of SA-βGal-positive cells expressed as a percentage of the total cell population in MDA-MB-231 cultures. Values represent mean ± SD. $^{a}P \leq 0.05$, $^{b}P \leq 0.01$, $^{c}P \leq 0.001$, $^{d}P \leq 0.0001$. iMSC-Exos: Exosomes derived from induced pluripotent stem cell-derived mesenchymal stem cells; BMSC-Exos: Exosomes derived from bone marrow mesenchymal stem cell; SFM: Serum-free medium.

DISCUSSION

MSCs possess remarkable regenerative properties, including their ability to migrate to injured tissues, differentiate into specific cell types, and secrete bioactive molecules such as chemokines, cytokines, and growth factors that facilitate tissue repair[20-22]. Among the various MSC sources, BMSCs have been widely studied for their therapeutic potential[21]. Increasing evidence indicates that the therapeutic effects of MSCs are largely mediated through paracrine signaling, particularly *via* EVs like Exos[23-25]. Importantly, Exos, including those derived from MSC, play a critical role in cancer biology, influencing tumor progression through mechanisms such as cell proliferation, metastasis, and resistance to chemotherapy[26,27].

Recently, iMSCs have emerged as a promising alternative to traditional MSCs, exhibiting improved survival, proliferation, and differentiation capabilities[8,28]. This study evaluated the effects of iMSC-Exos on pancreatic cancer (PANC1) and triple-negative breast cancer (MDA-MB-231) cells. Our results demonstrated that both iMSC-Exos and BMSC-Exos met the 2006 International Society for Cellular Therapy criteria for MSCs[29], including the presence of CD90, CD105, CD73, and CD44 human MSC surface markers, minimal expression of negative cocktail surface markers (CD34, CD11b, CD19, CD45, and HLA-DR), osteogenic and adipogenic differentiation potential, plastic adherence ability, and fibroblast-like morphology.

In our study the administration of Exos reduced proliferation in PANC1 and MDA-MB-231 cells with distinct variations in the duration and intensity of their effect. Unlike BMSC-Exos, iMSC-Exos maintained their antiproliferative effect at 48 hours in PANC1 cells. In contrast, both Exos types inhibited proliferation at 48 hours in MDA-MB-231 cells but not at 24 hours. Interestingly, Annexin V/PI staining showed no significant increase in apoptosis or necrosis in either cell line, suggesting that the antiproliferative effects of the Exos were mediated through non-apoptotic pathways. Moreover, HDFs showed no significant change in proliferation after treatment with either iMSC-Exos or BMSC-Exos. This absence of a proliferative response in non-malignant cells further emphasizes the potential selectivity of the exosomal effects. Such

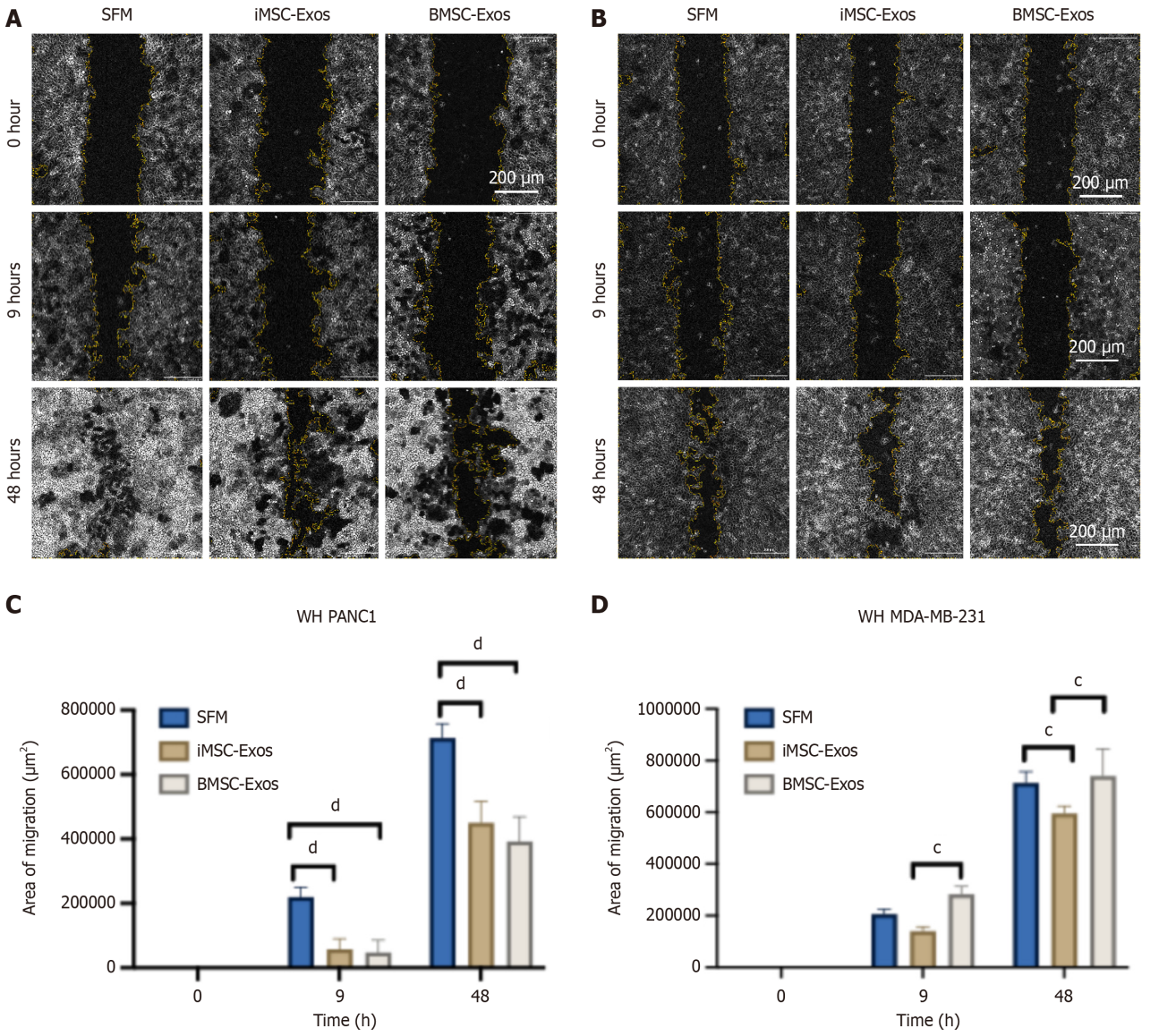

Figure 5 Invasion of PANC1 and MDA-MB-231 cells treated with exosomes. A and B: Representative images from the scratch assay illustrating wound closure in PANC1 (A) and MDA-MB-231 (B) cells treated with induced pluripotent stem cell-derived mesenchymal stem cell-derived exosomes or bone marrow mesenchymal stem cell-derived exosomes (scale bar = 200 μm); C and D: Quantitative analysis of wound area closure was conducted at 0 hour, 9 hours, and 48 hours post-scratch for PANC1 (C) and MDA-MB-231 (D) cells. Results are presented as mean ± SD. $^{c}P \leq 0.001$, $^{d}P \leq 0.0001$. iMSC-Exos: Exosomes derived from induced pluripotent stem cell-derived mesenchymal stem cells; BMSC-Exos: Exosomes derived from bone marrow mesenchymal stem cell; SFM: Serum-free medium.

selectivity suggests that the bioactive cargo of iMSC/BMSC-Exos preferentially modulates signaling pathways that are dysregulated in cancer cells and highlights the possibility of a therapeutic potential of iMSC/BMSC-Exos as a targeted cell-free anticancer approach with minimal effects on healthy cells.

Further analysis revealed an increased population of SA-βGal-positive cells in both cell lines treated with iMSC-Exos, whereas BMSC-Exos had divergent effects, reducing the burden of SA-βGal-positive cells in PANC1 cells but increasing it in MDA-MB-231 cells. Senescence, a stress-induced cellular response, is marked by a stable cell cycle arrest and the production of the SASP, which can exert both anti-tumor and tumor-promoting effects[30]. Our data suggests that the antiproliferative effects observed following Exos treatments are likely to be driven in part by increasing the percentage of SA-βGal-positive cells. Additionally, scratch assays demonstrated reduced invasion rates in PANC1 cells treated with both Exos types and in MDA-MB-231 cells treated with iMSC-Exos only, highlighting an additional anti-tumor effect of these Exos.

These contrasting effects highlight the cancer cell-dependent nature of MSC-Exos responses, aligning with the conflicting evidence reported in numerous studies regarding their role in cancer progression[13,16,31]. This variability is shaped by multiple factors, including the MSC source, culture conditions, EV isolation protocols, and the intrinsic biological differences among tumor models[32]. Notably, such conflicting effects have been observed both when EVs from different MSC sources act on the same cancer cells and when EVs from the same MSC source produce different outcomes in different cancer types[32]. Moreover, our data highlights the complexity of the senescent phenotype as a stress response in cancer cells. Cellular senescence in cancer can be triggered by a wide range of compounds acting

through different molecular pathways, resulting in diverse senescent phenotypes and variable experimental outcomes[33,34].

In this context the variation in senescence response observed between PANC1 and MDA-MB-231 cells following treatment with BMSC-Exos and iMSC-Exos is likely due to both differences in exosomal cargo and the distinct receptor or signaling profiles of the recipient cells. Notably, mutations in key senescence regulators like $p16^{Ink4a}$ have been reported in pancreatic cancer cells[35] and in triple-negative breast cancer cells such as MDA-MB-231[36,37], which may partly explain their altered response compared with normal cells. Furthermore, previous studies have reported that PANC1 is unlikely to be responsive to senescence-inducing therapy[38].

However, iMSC-Exos increased SA-βGal-positive cells in PANC1 cells, suggesting that they may carry specific effectors or miRNAs capable of modulating senescence more effectively, potentially by targeting distinct senescence pathways. Several miRNAs have been implicated in the regulation of senescence, functioning either as inhibitors (*e.g.*, miR-24, miR-17-5p, miR-20a/b, miR-106a/b) or inducers (*e.g.*, miR-16, miR-195, miR-107, miR-185)[39]. However, the cargo of iMSC-Exos has not been thoroughly investigated; existing studies have only provided preliminary characterization without detailing their molecular content[40], leaving open the question of which components contribute to the observed senescence response. Therefore, deeper molecular profiling of iMSC exosomal content is warranted, especially focusing on senescence-associated miRNAs and signaling proteins. Moreover, further analysis of additional senescence-associated markers is essential to fully elucidate the nature of tumor cell response to Exos.

Previous studies have shown that MSCs, including BMSCs, can either promote or inhibit pancreatic cancer growth through various signaling pathways[13]. For example, MSCs have been demonstrated to exert protumor effects through mechanisms such as chemokine (C-C motif) ligand 5 signaling[41], BxPc3 activation[42], or vascular endothelial growth factor production[43] while also exhibiting anti-tumor effects *via* interferon-β production[44]. Furthermore, Antoon *et al*[13] showed that BMSCs promoted pancreatic cancer growth through interleukin-6 production. Notably, interleukin-6 and vascular endothelial growth factor, among other factors, have been identified as components of Exos[45].

Moreover, studies on the effects of BMSC-Exos on triple negative breast cancer, particularly MDA-MB-231 cells, have yielded conflicting results. For instance, Hu *et al*[14] reported that BMSC-Exos suppressed MDA-231-MB stemness and metastasis *via* an ALKBH5-dependent mechanism. In contrast, a more recent study by Movahed *et al*[15] demonstrated that BMSC-Exos enhanced MDA-MB-231 stemness, likely by modulating metabolic pathways. The interaction between MSCs and cancer is complex and controversial. Some studies suggest that MSCs promote tumor growth while others indicate anti-tumor effects[46-48]. These divergent outcomes depend on variables like the MSC source, culture conditions, and passage number, which influence their biological properties[49].

Finally, the heterogeneity of MSC-Exos that is influenced by their parental cell origins and culture conditions[50,51] highlights the importance of considering the specific composition of Exos and the conditions under which they are generated when interpreting their cancer-related effects. This variability may explain the contrasting effects observed between MSCs and their Exos derivatives on cancer cells. However, despite the valuable insights offered in this study, further validation is required through the application of *in vivo* studies such xenograft models. Such models more effectively represent the complex physiological environment of the living system, incorporating key factors absent in the current *in vitro* system, including immune cell interactions, tumor stroma, and systemic influences. Additionally, this study did not assess the molecular cargo of the Exos, limiting our understanding of the mechanisms underlying the observed effects. Incorporating detailed cargo analysis alongside *in vivo* studies in future studies is essential to fully elucidate the biological mechanisms involved in the observed effects.

CONCLUSION

This study underscored the potential of iMSC-Exos as promising anti-cancer agents, particularly due to their ability to increase the number of SA-βGal-positive cells and inhibit invasion in specific cancer types. The findings highlighted the significant influence of the cellular source and culture conditions on the therapeutic efficacy of MSC-derived Exos. Future research should not only investigate the potential applications of iMSC-Exos across various cancer types but also elucidate the molecular mechanisms underlying these effects and validating the therapeutic potential in clinically relevant models.

ACKNOWLEDGEMENTS

We thank Professor Hatem Al-Kateib from School of Pharmacy, University of Jordan for helping with dynamic light scattering measurement.

FOOTNOTES

Author contributions: Ababneh NA and Awidi A conceptualized the study and supervised the study; Ababneh NA, Nashwan S, and Ismail MA carried out the experiments; Nashwan S and AlDiqs R wrote the initial draft of the manuscript; Ababneh NA, AlDiqs R, Abdulelah AA, Abu-Humaidan AHA, AlQirem L, Al-Abdallat K, Al-Qaisi T, and Saleh T revised and edited the manuscript; Ababneh NA, AlDiqs R, and Saleh T performed the formal analysis and results interpretation; All authors read and approved the final version of the publication.

Institutional review board statement: This study fully adhered to ethical standards and guidelines. It received approval from the Institutional Review Board, No. IRB-CTC/2-2021/06 at the Cell Therapy Center, University of Jordan in accordance with the Declaration of Helsinki.

Conflict-of-interest statement: All authors report no relevant conflicts of interest for this article.

Data sharing statement: The data that support the findings of this study are available from the corresponding author upon reasonable request.

Country of origin: Jordan

ORCID number: Nidaa A Ababneh 0000-0002-2155-3013.

S-Editor: Wang JJ
L-Editor: Filipodia
P-Editor: Wang CH

REFERENCES

1 **Kemp KC**, Hows J, Donaldson C. Bone marrow-derived mesenchymal stem cells. *Leuk Lymphoma* 2005; **46**: 1531-1544 [*RCA*] [PMID: 16236607 DOI: 10.1080/10428190500215076] [FullText]
2 **Maqsood M**, Kang M, Wu X, Chen J, Teng L, Qiu L. Adult mesenchymal stem cells and their exosomes: Sources, characteristics, and application in regenerative medicine. *Life Sci* 2020; **256**: 118002 [*RCA*] [PMID: 32585248 DOI: 10.1016/j.lfs.2020.118002] [FullText]
3 **Liao HJ**, Hsu PN. Immunomodulatory effects of extracellular vesicles from mesenchymal stromal cells: Implication for therapeutic approach in autoimmune diseases. *Kaohsiung J Med Sci* 2024; **40**: 520-529 [*RCA*] [PMID: 38712483 DOI: 10.1002/kjm2.12841] [FullText]
4 **Cerrotti G**, Buratta S, Latella R, Calzoni E, Cusumano G, Bertoldi A, Porcellati S, Emiliani C, Urbanelli L. Hitting the target: cell signaling pathways modulation by extracellular vesicles. *Extracell Vesicles Circ Nucl Acids* 2024; **5**: 527-552 [*RCA*] [PMID: 39697631 DOI: 10.20517/evcna.2024.16] [FullText]
5 **Ullah I**, Subbarao RB, Rho GJ. Human mesenchymal stem cells - current trends and future prospective. *Biosci Rep* 2015; **35**: e00191 [*RCA*] [PMID: 25797907 DOI: 10.1042/BSR20150025] [FullText] [Full Text(PDF)]
6 **Chen LY**, Kao TW, Chen CC, Niaz N, Lee HL, Chen YH, Kuo CC, Shen YA. Frontier Review of the Molecular Mechanisms and Current Approaches of Stem Cell-Derived Exosomes. *Cells* 2023; **12**: 1018 [*RCA*] [PMID: 37048091 DOI: 10.3390/cells12071018] [FullText]
7 **Choudhery MS**, Arif T, Mahmood R, Harris DT. Stem Cell-Based Acellular Therapy: Insight into Biogenesis, Bioengineering and Therapeutic Applications of Exosomes. *Biomolecules* 2024; **14**: 792 [*RCA*] [PMID: 39062506 DOI: 10.3390/biom14070792] [FullText] [Full Text(PDF)]
8 **Sabapathy V**, Kumar S. hiPSC-derived iMSCs: NextGen MSCs as an advanced therapeutically active cell resource for regenerative medicine. *J Cell Mol Med* 2016; **20**: 1571-1588 [*RCA*] [PMID: 27097531 DOI: 10.1111/jcmm.12839] [FullText] [Full Text(PDF)]
9 **Liu G**, David BT, Trawczynski M, Fessler RG. Advances in Pluripotent Stem Cells: History, Mechanisms, Technologies, and Applications. *Stem Cell Rev Rep* 2020; **16**: 3-32 [*RCA*] [PMID: 31760627 DOI: 10.1007/s12015-019-09935-x] [FullText] [Full Text(PDF)]
10 **Hu GW**, Li Q, Niu X, Hu B, Liu J, Zhou SM, Guo SC, Lang HL, Zhang CQ, Wang Y, Deng ZF. Exosomes secreted by human-induced pluripotent stem cell-derived mesenchymal stem cells attenuate limb ischemia by promoting angiogenesis in mice. *Stem Cell Res Ther* 2015; **6**: 10 [*RCA*] [PMID: 26268554 DOI: 10.1186/scrt546] [FullText] [Full Text(PDF)]
11 **Kim S**, Lee SK, Kim H, Kim TM. Exosomes Secreted from Induced Pluripotent Stem Cell-Derived Mesenchymal Stem Cells Accelerate Skin Cell Proliferation. *Int J Mol Sci* 2018; **19**: 3119 [*RCA*] [PMID: 30314356 DOI: 10.3390/ijms19103119] [FullText] [Full Text(PDF)]
12 **Choi EW**, Lim IR, Park JH, Song J, Choi B, Kim S. Exosomes derived from mesenchymal stem cells primed with disease-condition-serum improved therapeutic efficacy in a mouse rheumatoid arthritis model *via* enhanced TGF-β1 production. *Stem Cell Res Ther* 2023; **14**: 283 [*RCA*] [PMID: 37794417 DOI: 10.1186/s13287-023-03523-0] [FullText]
13 **Antoon R**, Wang XH, Saleh AH, Warrington J, Hedley DW, Keating A. Pancreatic cancer growth promoted by bone marrow mesenchymal stromal cell-derived IL-6 is reversed predominantly by IL-6 blockade. *Cytotherapy* 2022; **24**: 699-710 [*RCA*] [PMID: 35473998 DOI: 10.1016/j.jcyt.2021.12.005] [FullText]
14 **Hu Y**, Liu H, Xiao X, Yu Q, Deng R, Hua L, Wang J, Wang X. Bone Marrow Mesenchymal Stem Cell-Derived Exosomes Inhibit Triple-Negative Breast Cancer Cell Stemness and Metastasis *via* an ALKBH5-Dependent Mechanism. *Cancers (Basel)* 2022; **14**: 6059 [*RCA*] [PMID: 36551544 DOI: 10.3390/cancers14246059] [FullText] [Full Text(PDF)]
15 **Movahed ZG**, Mansouri K, Mohsen AH, Matin MM. Bone marrow mesenchymal stem cells enrich breast cancer stem cell population *via* targeting metabolic pathways. *Med Oncol* 2025; **42**: 90 [*RCA*] [PMID: 40045066 DOI: 10.1007/s12032-025-02632-5] [FullText]
16 **Ababneh NA**, Aldiqs R, Nashwan S, Ismail MA, Barham R, Al Hadidi S, Alrefae A, Alhallaq FK, Abu-Humaidan AH, Saleh T, Awidi A. Distinct anticancer properties of exosomes from induced mesenchymal stem cells vs. bone marrow-derived stem cells in MCF7 and A549 models. *Biomed Rep* 2025; **23**: 116 [*RCA*] [PMID: 40420975 DOI: 10.3892/br.2025.1994] [FullText] [Full Text(PDF)]
17 **Ababneh NA**, Al-Kurdi B, Jamali F, Awidi A. A comparative study of the capability of MSCs isolated from different human tissue sources to differentiate into neuronal stem cells and dopaminergic-like cells. *PeerJ* 2022; **10**: e13003 [*RCA*] [PMID: 35341051 DOI:

10.7717/peerj.13003] [FullText] [Full Text(PDF)]

18 **Ababneh NA**, Al-Kurdi B, Barham R, Ali D, Sharar N, Abuarqoub D, Jafar H, Salah B, Awidi A. Derivation of three human induced pluripotent stem cell lines (JUCTCi014-A, JUCTCi015-A, JUCTCi016-A) from mesenchymal stem cells (MSCs) derived from bone marrow, adipose tissue and Wharton's jelly samples. *Stem Cell Res* 2020; **49**: 102000 [*RCA*] [PMID: 33010679 DOI: 10.1016/j.scr.2020.102000] [Full Text]

19 **Wang S**, Hou Y, Li X, Song Z, Sun B, Li X, Zhang H. Comparison of exosomes derived from induced pluripotent stem cells and mesenchymal stem cells as therapeutic nanoparticles for treatment of corneal epithelial defects. *Aging (Albany NY)* 2020; **12**: 19546-19562 [*RCA*] [PMID: 33049719 DOI: 10.18632/aging.103904] [FullText] [Full Text(PDF)]

20 **Abdal Dayem A**, Lee SB, Kim K, Lim KM, Jeon TI, Seok J, Cho AS. Production of Mesenchymal Stem Cells Through Stem Cell Reprogramming. *Int J Mol Sci* 2019; **20**: 1922 [*RCA*] [PMID: 31003536 DOI: 10.3390/ijms20081922] [FullText] [Full Text(PDF)]

21 **Fu X**, Liu G, Halim A, Ju Y, Luo Q, Song AG. Mesenchymal Stem Cell Migration and Tissue Repair. *Cells* 2019; **8**: 784 [*RCA*] [PMID: 31357692 DOI: 10.3390/cells8080784] [FullText] [Full Text(PDF)]

22 **Naji A**, Eitoku M, Favier B, Deschaseaux F, Rouas-Freiss N, Suganuma N. Biological functions of mesenchymal stem cells and clinical implications. *Cell Mol Life Sci* 2019; **76**: 3323-3348 [*RCA*] [PMID: 31055643 DOI: 10.1007/s00018-019-03125-1] [FullText]

23 **Keshtkar S**, Azarpira N, Ghahremani MH. Mesenchymal stem cell-derived extracellular vesicles: novel frontiers in regenerative medicine. *Stem Cell Res Ther* 2018; **9**: 63 [*RCA*] [PMID: 29523213 DOI: 10.1186/s13287-018-0791-7] [FullText] [Full Text(PDF)]

24 **Watanabe Y**, Tsuchiya A, Terai S. The development of mesenchymal stem cell therapy in the present, and the perspective of cell-free therapy in the future. *Clin Mol Hepatol* 2021; **27**: 70-80 [*RCA*] [PMID: 33317249 DOI: 10.3350/cmh.2020.0194] [FullText] [Full Text(PDF)]

25 **Phetfong J**, Tawonsawatruk T, Kamprom W, Ontong P, Tanyong D, Borwornpinyo S, Supokawej A. Bone marrow-mesenchymal stem cell-derived extracellular vesicles affect proliferation and apoptosis of leukemia cells in vitro. *FEBS Open Bio* 2022; **12**: 470-479 [*RCA*] [PMID: 34907674 DOI: 10.1002/2211-5463.13352] [FullText] [Full Text(PDF)]

26 **Sohrabi B**, Dayeri B, Zahedi E, Khoshbakht S, Nezamabadi Pour N, Ranjbar H, Davari Nejad A, Noureddini M, Alani B. Mesenchymal stem cell (MSC)-derived exosomes as novel vehicles for delivery of miRNAs in cancer therapy. *Cancer Gene Ther* 2022; **29**: 1105-1116 [*RCA*] [PMID: 35082400 DOI: 10.1038/s41417-022-00427-8] [FullText]

27 **Lin Z**, Wu Y, Xu Y, Li G, Li Z, Liu T. Mesenchymal stem cell-derived exosomes in cancer therapy resistance: recent advances and therapeutic potential. *Mol Cancer* 2022; **21**: 179 [*RCA*] [PMID: 36100944 DOI: 10.1186/s12943-022-01650-5] [FullText] [Full Text(PDF)]

28 **Wruck W**, Graffmann N, Spitzhorn LS, Adjaye J. Human Induced Pluripotent Stem Cell-Derived Mesenchymal Stem Cells Acquire Rejuvenation and Reduced Heterogeneity. *Front Cell Dev Biol* 2021; **9**: 717772 [*RCA*] [PMID: 34604216 DOI: 10.3389/fcell.2021.717772] [FullText] [Full Text(PDF)]

29 **Dominici M**, Le Blanc K, Mueller I, Slaper-Cortenbach I, Marini F, Krause D, Deans R, Keating A, Prockop Dj, Horwitz E. Minimal criteria for defining multipotent mesenchymal stromal cells. The International Society for Cellular Therapy position statement. *Cytotherapy* 2006; **8**: 315-317 [*RCA*] [PMID: 16923606 DOI: 10.1080/14653240600855905] [FullText]

30 **Schmitt CA**, Wang B, Demaria M. Senescence and cancer - role and therapeutic opportunities. *Nat Rev Clin Oncol* 2022; **19**: 619-636 [*RCA*] [PMID: 36045302 DOI: 10.1038/s41571-022-00668-4] [FullText] [Full Text(PDF)]

31 **Yang E**, Jing S, Wang Y, Wang H, Rodriguez R, Wang Z. The Role of Mesenchymal Stem Cells and Exosomes in Tumor Development and Targeted Antitumor Therapies. *Stem Cells Int* 2023; **2023**: 7059289 [*RCA*] [PMID: 36824409 DOI: 10.1155/2023/7059289] [FullText]

32 **Tan TT**, Lai RC, Padmanabhan J, Sim WK, Choo ABH, Lim SK. Assessment of Tumorigenic Potential in Mesenchymal-Stem/Stromal-Cell-Derived Small Extracellular Vesicles (MSC-sEV). *Pharmaceuticals (Basel)* 2021; **14**: 345 [*RCA*] [PMID: 33918628 DOI: 10.3390/ph14040345] [FullText] [Full Text(PDF)]

33 **Petrova NV**, Velichko AK, Razin SV, Kantidze OL. Small molecule compounds that induce cellular senescence. *Aging Cell* 2016; **15**: 999-1017 [*RCA*] [PMID: 27628712 DOI: 10.1111/acel.12518] [FullText] [Full Text(PDF)]

34 **Hernandez-Segura A**, de Jong TV, Melov S, Guryev V, Campisi J, Demaria M. Unmasking Transcriptional Heterogeneity in Senescent Cells. *Curr Biol* 2017; **27**: 2652-2660.e4 [*RCA*] [PMID: 28844647 DOI: 10.1016/j.cub.2017.07.033] [FullText]

35 **Voutsadakis IA**. Mutations of p53 associated with pancreatic cancer and therapeutic implications. *Ann Hepatobiliary Pancreat Surg* 2021; **25**: 315-327 [*RCA*] [PMID: 34402431 DOI: 10.14701/ahbps.2021.25.3.315] [FullText] [Full Text(PDF)]

36 **Hui R**, Macmillan RD, Kenny FS, Musgrove EA, Blamey RW, Nicholson RI, Robertson JF, Sutherland RL. INK4a gene expression and methylation in primary breast cancer: overexpression of p16INK4a messenger RNA is a marker of poor prognosis. *Clin Cancer Res* 2000; **6**: 2777-2787 [*RCA*] [PMID: 10914724] [FullText]

37 **de Paula B**, Kieran R, Koh SSY, Crocamo S, Abdelhay E, Muñoz-Espín D. Targeting Senescence as a Therapeutic Opportunity for Triple-Negative Breast Cancer. *Mol Cancer Ther* 2023; **22**: 583-598 [*RCA*] [PMID: 36752780 DOI: 10.1158/1535-7163.MCT-22-0643] [FullText] [Full Text(PDF)]

38 **Abu-Humaidan AH**, Ismail MA, Ahmad FM, Al Shboul S, Barham R, Tadros JS, Alhesa A, El-Sadoni M, Alotaibi MR, Ababneh NA, Saleh T. Therapy-induced senescent cancer cells exhibit complement activation and increased complement regulatory protein expression. *Immunol Cell Biol* 2024; **102**: 240-255 [*RCA*] [PMID: 38265162 DOI: 10.1111/imcb.12727] [FullText]

39 **Xu D**, Tahara H. The role of exosomes and microRNAs in senescence and aging. *Adv Drug Deliv Rev* 2013; **65**: 368-375 [*RCA*] [PMID: 22820533 DOI: 10.1016/j.addr.2012.07.010] [FullText]

40 **Nashwan S**, Ismail MA, Saleh T, Al Hadidi S, Alwohoush E, Sarhan M, Harfeil NA, Awidi A, Ababneh NA. Comparative analysis of extracellular vesicles from induced and adipose-derived Mesenchymal Stem Cells: Implications for regenerative medicine. *PLoS One* 2025; **20**: e0325065 [*RCA*] [PMID: 40465768 DOI: 10.1371/journal.pone.0325065] [FullText] [Full Text(PDF)]

41 **Makinoshima H**, Dezawa M. Pancreatic cancer cells activate CCL5 expression in mesenchymal stromal cells through the insulin-like growth factor-I pathway. *FEBS Lett* 2009; **583**: 3697-3703 [*RCA*] [PMID: 19874825 DOI: 10.1016/j.febslet.2009.10.061] [FullText]

42 **Saito K**, Sakaguchi M, Maruyama S, Iioka H, Putranto EW, Sumardika IW, Tomonobu N, Kawasaki T, Homma K, Kondo E. Stromal mesenchymal stem cells facilitate pancreatic cancer progression by regulating specific secretory molecules through mutual cellular interaction. *J Cancer* 2018; **9**: 2916-2929 [*RCA*] [PMID: 30123360 DOI: 10.7150/jca.24415] [FullText] [Full Text(PDF)]

43 **Beckermann BM**, Kallifatidis G, Groth A, Frommhold D, Apel A, Mattern J, Salnikov AV, Moldenhauer G, Wagner W, Diehlmann A, Saffrich R, Schubert M, Ho AD, Giese N, Büchler MW, Friess H, Büchler P, Herr I. VEGF expression by mesenchymal stem cells contributes to angiogenesis in pancreatic carcinoma. *Br J Cancer* 2008; **99**: 622-631 [*RCA*] [PMID: 18665180 DOI: 10.1038/sj.bjc.6604508] [FullText] [Full Text(PDF)]

44 **Kidd S**, Caldwell L, Dietrich M, Samudio I, Spaeth EL, Watson K, Shi Y, Abbruzzese J, Konopleva M, Andreeff M, Marini FC. Mesenchymal stromal cells alone or expressing interferon-beta suppress pancreatic tumors in vivo, an effect countered by anti-inflammatory treatment. *Cytotherapy* 2010; **12**: 615-625 [*RCA*] [PMID: 20230221 DOI: 10.3109/14653241003631815] [FullText]

45 **Jung HH**, Kim JY, Lim JE, Im YH. Cytokine profiling in serum-derived exosomes isolated by different methods. *Sci Rep* 2020; **10**: 14069 [*RCA*] [PMID: 32826923 DOI: 10.1038/s41598-020-70584-z] [FullText] [Full Text(PDF)]

46 **Cheshomi H**, Matin MM. Exosomes and their importance in metastasis, diagnosis, and therapy of colorectal cancer. *J Cell Biochem* 2019; **120**: 2671-2686 [*RCA*] [PMID: 30246315 DOI: 10.1002/jcb.27582] [FullText]

47 **Brossa A**, Fonsato V, Grange C, Tritta S, Tapparo M, Calvetti R, Cedrino M, Fallo S, Gontero P, Camussi G, Bussolati B. Extracellular vesicles from human liver stem cells inhibit renal cancer stem cell-derived tumor growth in vitro and in vivo. *Int J Cancer* 2020; **147**: 1694-1706 [*RCA*] [PMID: 32064610 DOI: 10.1002/ijc.32925] [FullText] [Full Text(PDF)]

48 **Weng Z**, Zhang B, Wu C, Yu F, Han B, Li B, Li L. Therapeutic roles of mesenchymal stem cell-derived extracellular vesicles in cancer. *J Hematol Oncol* 2021; **14**: 136 [*RCA*] [PMID: 34479611 DOI: 10.1186/s13045-021-01141-y] [FullText] [Full Text(PDF)]

49 **Yi N**, Zeng Q, Zheng C, Li S, Lv B, Wang C, Li C, Jiang W, Liu Y, Yang Y, Yan T, Xue J, Xue Z. Functional variation among mesenchymal stem cells derived from different tissue sources. *PeerJ* 2024; **12**: e17616 [*RCA*] [PMID: 38952966 DOI: 10.7717/peerj.17616] [FullText] [Full Text(PDF)]

50 **Almeria C**, Kreß S, Weber V, Egger D, Kasper C. Heterogeneity of mesenchymal stem cell-derived extracellular vesicles is highly impacted by the tissue/cell source and culture conditions. *Cell Biosci* 2022; **12**: 51 [*RCA*] [PMID: 35501833 DOI: 10.1186/s13578-022-00786-7] [Full Text] [Full Text(PDF)]

51 **Luo Y**, Li Z, Wang X, Wang J, Duan X, Li R, Peng Y, Ye Q, He Y. Characteristics of culture-condition stimulated exosomes or their loaded hydrogels in comparison with other extracellular vesicles or MSC lysates. *Front Bioeng Biotechnol* 2022; **10**: 1016833 [*RCA*] [PMID: 36185445 DOI: 10.3389/fbioe.2022.1016833] [FullText] [Full Text(PDF)]

Published by **Baishideng Publishing Group Inc**
7041 Koll Center Parkway, Suite 160, Pleasanton, CA 94566, USA
Telephone: +1-925-3991568
E-mail: office@baishideng.com
Help Desk: https://www.f6publishing.com/helpdesk
https://www.wjgnet.com